ELSEVIER

Fuel Processing Technology 87 (2006) 1031 – 1036

FUEL PROCESSING TECHNOLOGY

www.elsevier.com/locate/fuproc

Artificial neural network predictions of polycyclic aromatic hydrocarbon formation in premixed *n*-heptane flames

Fikret Inal *

Department of Chemical Engineering, Izmir Institute of Technology, Gulbahce-Urla, 35430 Izmir, Turkey

Received 16 February 2006; received in revised form 28 July 2006; accepted 3 August 2006

Abstract

Polycyclic aromatic hydrocarbon formation in combustion systems has received considerable attention because of its health effects. The feed-forward, multi-layer perceptron type artificial neural networks with back-propagation learning were used to predict the total PAH amount in atmospheric pressure, premixed *n*-heptane and *n*-heptane/oxygenate flames. MTBE and ethanol were used as fuel oxygenates. The total fifty-four data sets were divided into three groups: training, cross-validation, and testing. The different network architectures were tested and the best predictions were obtained for a network of one hidden layer with five neurons. The transfer function was sigmoid function. The mean square and mean absolute errors were 10.52 and 2.60 ppm for the testing set, respectively. The correlation coefficient (R^2) was 0.98. The results also showed that the total PAH amount was significantly influenced by the changes in equivalence ratio, presence of fuel oxygenates, and mole fractions of C_4 species.

Keywords: Neural network; PAH; Premixed flame

1. Introduction

Combustion systems generally produce measurable amounts of polycyclic aromatic hydrocarbons (PAH) due to incomplete combustion of hydrocarbon fuels. Although PAH are considered trace components in most combustion systems, low level exposure to these combustion-produced compounds may increase the incidence of cancer and genetic defects. PAH are the largest class of chemical carcinogens known. A recent review on cancer risk from occupational and environmental exposure to PAH shows that heavy exposure to PAH causes a substantial risk of lung, skin, and bladder cancer [1]. The major sources of PAH emissions are stationary sources (e.g., residential heating, power and heat generation, industry, and incineration) and mobile sources (e.g., gasoline-engine automobiles and diesel-engine automobiles) [2].

The amounts of PAH emitted from gasoline [3–7] and diesel [3,7–11] engines have been studied extensively in the literature. Since *n*-heptane is a component of commercial gasoline and one of the primary reference fuels for the determination of octane number, it has been used as a model compound for the alkane components of practical hydrocarbon fuels in many combustion studies. The formation of PAH in premixed *n*-heptane flame at an equivalence ratio (ϕ) of 2.05 has been investigated by Westmoreland et al. [12]. The most abundant compound was acenaphthylene. Peterca and Marconi [13] have reported acenaphthylene and naphthalene as major PAH species in laminar diffusion flames of *n*-heptane. The concentration profiles of stable species and free radicals in low-pressure (6.0 kPa), laminar, premixed *n*-heptane flames have been reported by Doute et al. [14] for equivalence ratios of $0.7 \leq \phi \leq 2.0$ using molecular beam mass spectrometry. El Bakali et al. [15] and Ingemarsson et al. [16] have carried out quartz microprobe sampling and GC/MS analysis for the low-molecular-weight species (e.g., up to benzene) concentration profiles in atmospheric pressure, premixed *n*-heptane flames at equivalence ratios of 1.9 and 1.0, respectively. Recently, we [17] have investigated the PAH formation in fuel rich ($\phi = 1.97$ and 2.10) laminar, premixed *n*-heptane flames. The concentrations of aromatic and PAH compounds were increased with increasing equivalence ratio. Acenaphthylene and naphthalene were the most abundant PAH species.

* Tel.: +90 232 750 6654; fax: +90 232 750 6645.
E-mail address: fikretinal@iyte.edu.tr.

0378-3820/$ - see front matter © 2006 Elsevier B.V. All rights reserved.
doi:10.1016/j.fuproc.2006.08.002

Fuel oxygenates are used to reduce mobile source emissions. Ethers (e.g., MTBE, ETBE) and alcohols (e.g., methanol, ethanol) are preferred as oxygenate additives in gasoline. Ethers have low heat of vaporization and can be blended at the refinery. In contrast, alcohols have higher heat of vaporization. However, they can supply higher levels of oxygen at lower concentrations. In addition, ethanol is the only renewable fuel oxygenate. The effects of fuel oxygenate on PAH formation in *n*-heptane flames have been investigated by Inal and Senkan [18,19].

Detailed chemical reaction mechanisms have been used to predict the species concentration profiles, ignition delay times, and laminar burning velocities in *n*-heptane oxidation [20–27]. These mechanisms include a large number of species in a large number of elementary reactions, and require thermodynamic, transport, and chemical kinetic data. On the other hand, artificial neural network (ANN) modeling technique has also been applied successfully to predict the concentrations of various environmental pollutants. Elkamel et al. [28] have used an ANN model to predict ground-level ozone concentrations as a function of meteorological conditions and precursor concentrations (i.e., methane, carbon monoxide, carbon dioxide, nitrogen oxide, nitrogen dioxide, sulfur dioxide, non-methane hydrocarbons, and dust). PAH [29] and particulate [30] emissions from a passenger car diesel engine were studied as functions of fuel parameters and operation conditions using ANNs. The exhaust carbon monoxide, hydrocarbons, nitrogen oxides, and particulate emissions from a single-cylinder diesel engine have also been modeled by the ANN approach [31]. Inal et al. [32] have developed three-layer, feed-forward type ANNs to investigate soot formation in premixed hydrocarbon flames. In a recent study, Jensen et al. [33] have used an ANN model to predict mercury speciation (elemental, oxidized, and particulate) from power plants.

The objective of this study was to develop an ANN model to predict the total PAH amount in atmospheric pressure, laminar, premixed flames of *n*-heptane/oxygen/argon and *n*-heptane/oxygen/oxygenate/argon as functions of flame parameters (e.g., distance from the burner surface and flame temperature), equivalence ratio, amount of oxygenate in the fuel blend, and the concentrations of PAH precursors (i.e., low-molecular-weight reaction products and one-ring compounds). MTBE and ethanol were used as fuel oxygenates since they are the most common oxygenates currently used in gasoline.

2. Experimental

The details of the experimental setup used for data acquisition have been given elsewhere [17,18]. Therefore, only a brief description will be presented here. Atmospheric pressure, laminar, premixed, flat-flames of *n*-heptane/oxygen/argon and *n*-heptane/oxygen/oxygenate/argon were stabilized over a 50-mm diameter porous bronze burner. Mole fraction profiles of species were obtained by the direct GC/MS analysis of flame samples using a heated quartz microprobe. For the quantifications of species either direct-calibration standards (Matheson Gas, Sigma Aldrich) or ionization cross-section method [34] was used. An accuracy of about ±15% was estimated for the mole fractions of species determined by direct calibration. Ionization cross-section method has been reported to be accurate within a factor of 2 [34].

The flame temperatures were measured with a silica-coated 0.075 mm Pt–13% Rh/Pt thermocouple. Temperatures used in this study correspond to direct thermocouple readings and were not corrected for radiation losses.

3. ANN model

Artificial neural networks are interconnected parallel systems consisting of simple processing elements, neurons. In this study, a feed-forward, multi-layer perceptron (MLP) type of ANNs as shown in Fig. 1, was considered for the prediction of total PAH amount in a premixed combustion of *n*-heptane. MLP is the most widely used neural network architecture and consists of an input layer, one or more hidden layers, and an output layer. The neurons in the input layer receive input quantities and pass them on to the hidden layer neurons without any computation. The hidden layer neurons calculate their inputs by adding up the weighted inputs received from each neuron in the previous layer. The connections between the neurons are called weights. Weights determine the strength of the input signal. The outputs of the hidden neurons are calculated by passing the sum of the weighted inputs received on through a non-linear transfer or activation function. The output neurons perform the same operations as those of hidden neurons. The hyperbolic tangent and sigmoid transfer functions have been tested in one- and two-hidden layer networks.

Learning of the ANN is accomplished through the training procedure. The back-propagation algorithm, the most commonly used supervised learning algorithm in MLP, was utilized in this study. In the training procedure, the information is processed in the forward direction from input layer to the hidden layer and then to the output layer (feed-forward) to obtain the output of the network. The desired output at each output neuron is compared with the network output, and the difference or error is computed. The error function has the following form [35]:

$$E = \sum_k \sum_n (d_{nk} - y_{nk})^2 \quad (1)$$

where k is an index over the system output, n is an index over the input patterns, d is a component of the desired or target output

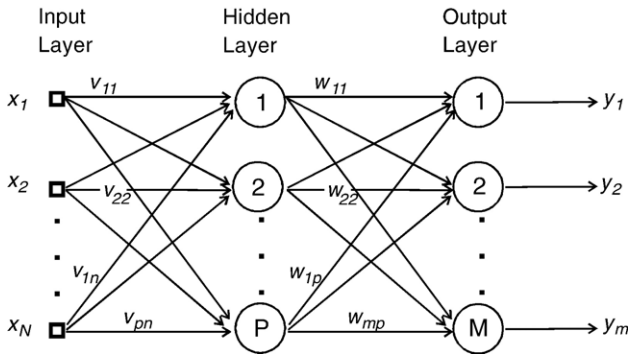

Fig. 1. Feed-forward, multi-layer perceptron type artificial neural networks.

Table 1
Pre-combustion compositions of the flames

	ϕ=1.97	ϕ=2.10
n-Heptane flames		
n-Heptane (mol%)	5.33	5.50
Oxygen (mol%)	29.70	28.79
n-Heptane/MTBE flames		
n-Heptane (mol%)	4.55	4.70
Oxygen (mol%)	29.21	28.28
Oxygen in *n*-heptane/MTBE blend (wt.%)	2.7	2.7
n-Heptane/ethanol flames		
n-Heptane (mol%)	4.91	5.07
Oxygen (mol%)	29.08	28.07
Oxygen in *n*-heptane/ethanol blend (wt.%)	2.7	2.7

vector **D**, and y is a component of the network output vector **Y**. The error is propagated in the backward direction from the output layer to the input layer (back-propagation), and it is minimized by adjusting the connection weights. Batch training mode has been used to update the weights since it is more stable and efficient. In batch training, weights are updated after the presentation of the entire training set. The weight update procedure becomes an important issue especially for the non-convex performance surfaces. To avoid the training process being trapped in local minima or saddle points in search of optimum weights, adaptive weight update procedure (Delta bar delta) has been applied [35]. This procedure speeds up the training by providing high learning rates when the learning curve is flat and low learning rates when the learning curve oscillates. For the best generalization performance of the network, the training data set was divided into two groups: training and cross-validation sets, and the training was stopped when the cross-validation error began to increase. The connection weights of the network were automatically saved at this point, and used later in the testing procedure. After the training, the next step in ANN development is testing. In testing, the performance of the trained network has been verified with testing data set that the network was not trained with.

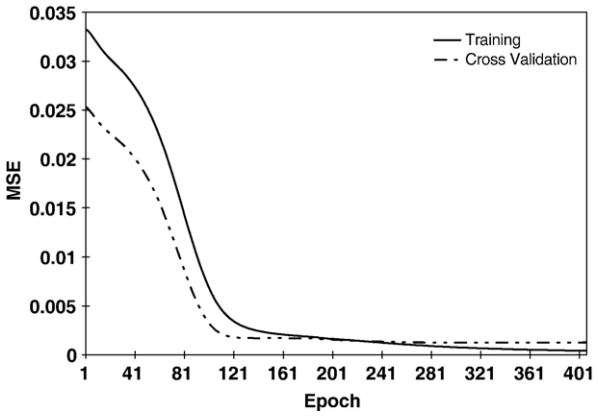

Fig. 2. Learning curves for training and cross-validation sets.

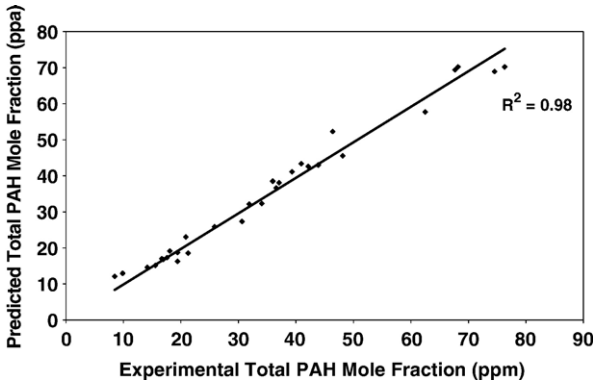

Fig. 3. Experimental and ANN predicted total PAH amounts for the training set.

NeuroSolutions (Version 4, NeuroDimension Inc.) software was used to build ANN models in this study.

4. Results and discussion

The pre-combustion compositions of the flames are given in Table 1. Ar dilution was kept at about 65% in all the flames. The oxygen weight percent in *n*-heptane/oxygenate mixtures was 2.7 for each oxygenate studied. The equivalence ratios (ϕ=1.97 and 2.10; ϕ=(Fuel/Oxygen)$_{actual}$/(Fuel/Oxygen)$_{stoich.}$) and compositions were determined to obtain stable flames that produce a measurable amount of PAH. The quartz sampling probe was plugged at higher equivalence ratios due to excessive soot formation, thus requiring the early termination of the experiments. On the other hand, the flames did not produce enough PAH at low equivalence ratios.

The distance from the burner surface, flame temperature, equivalence ratio, concentrations of MTBE and ethanol in the reactant mixtures, and mole fractions of acetylene, 1,3-propadiene, diacetylene, vinylacetylene, benzene, toluene, and phenylacetylene were used as input parameters. The output parameter was the total PAH mole fraction, which includes the sum of the mole fractions of seven PAH compounds: naphthalene, acenaphthylene, phenanthrene, 4H-cyclopenta[def]-phenanthrene, fluoranthene, pyrene, and cyclopenta[cd]pyrene. Benzene was the most abundant aromatic compound and acenaphthylene and naphthalene were the most abundant PAH compounds in all the flames studied [18].

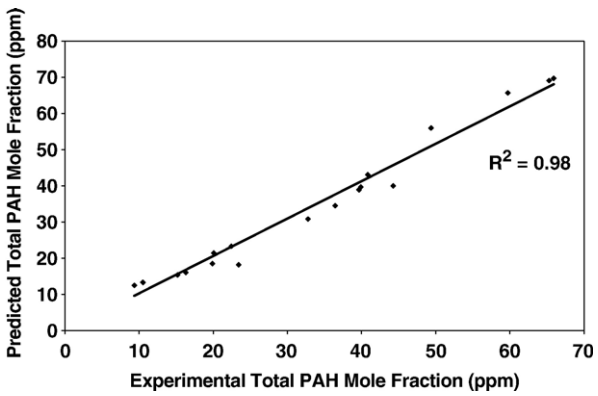

Fig. 4. Experimental and ANN predicted total PAH amounts for the testing set.

Table 2
Performance of the network on training and testing sets

Performance	Training	Testing
MSE	7.30	10.52
MAE	2.05	2.60
Min abs error	0.05	0.19
Max abs error	6.11	6.62
R^2	0.98	0.98

Fifty-four data sets obtained from six flames were divided into three groups: training, cross-validation, and testing, each containing 30 (~56%), 6 (~11%), and 18 (~33%) sets, respectively. Care has been taken to have representative data in the training set since ANN performs better when predicting output parameter within the limits of the training data. Both the temperature and species concentration profiles within a few millimeters above the burner surface are subject to considerable probe–burner surface interactions thus were not used in modeling activities. The concentration and temperature data correspond to 2 mm–10 mm above the burner surface. The different neural network architectures were tested to obtain the best performance on total PAH predictions. The network parameters to be optimized were the number of hidden layer, number of neurons in each hidden layer, and type of transfer function. We have tested one- and two-hidden layer networks with two to ten processing elements. For each case sigmoid and hyperbolic tangent transfer functions were tried. Sigmoid function produces output values between [0, 1] while the hyperbolic tangent produces values between [−1, 1]. These two functions are continuous and differentiable, which will be very important in weight adaptation during the training process.

After extensive trial and error runs, the best performance was obtained with one-hidden layer network with five neurons (network architecture; 12–5–1). The transfer function was sigmoid function. The increase in the number of hidden layer and the number of neurons in each hidden layer did not significantly improve the performance of the network. We preferred low complexity network since the larger networks require more free parameters to solve a given problem and may over fit the data. In addition, the complex networks need more training and testing time. The ANN results are given for the (12–5–1) network architecture.

The learning curves for training and cross-validation sets are given in Fig. 2. Mean square errors (MSE) decrease initially both for the training and cross-validation sets. However, the cross-validation MSE starts to increase when the network begins to over train the data. The ANN model automatically saves the connection weights of the network when the cross-validation MSE reaches a minimum value, and utilizes them in the testing procedure.

Table 3
Sensitivity factors for the concentration related input parameters

Input	Sensitivity factor
Equivalence ratio	41.32
MTBE	10.48
Ethanol	8.57
C_8H_6	0.65
C_7H_8	0.35
C_6H_6	0.28
C_4H_4	4.96
C_4H_2	2.95
C_3H_4	0.39
C_2H_2	0.38

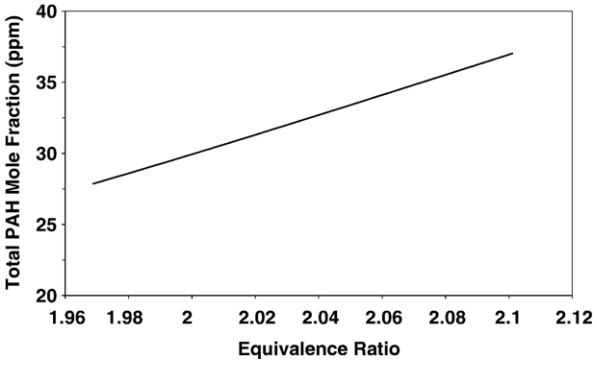

Fig. 5. Effect of equivalence ratio on total PAH amount.

The predicted and experimental total PAH mole fractions are shown in Fig. 3 for the training set. There was a good agreement between the ANN predictions and experimental data with a correlation coefficient of 0.98. The correlation coefficient was also 0.98 for the testing data set (Fig. 4). The performance of the network on training and testing sets is summarized in Table 2. For the training set, MSE and mean absolute error (MAE) were 7.30 ppm and 2.05 ppm, respectively. The ANN model also exhibited satisfactory performance for the testing set. The MSE and MAE were 10.52 ppm and 2.60 ppm, respectively. The similar values of MSE, MAE, and R^2 for training and testing sets indicate that the network did not over train or memorize the data.

There are several mechanisms proposed for the formation and growth of PAH in flames. One of the important steps in these mechanisms is the formation of single-ring aromatics for the combustion of aliphatic fuels. Frenklach and Wang [36] suggested that the formation of the first aromatic ring in flames of non-aromatic fuels usually begins with vinyl addition to acetylene. Vinylacetylene is formed at high temperatures, and followed by acetylene addition to n-C_4H_3, radical formed by the H-abstraction from the vinylacetylene. At low temperatures the vinyl addition to acetylene forms n-C_4H_5, which upon addition of acetylene produces benzene. The H-abstraction reaction and

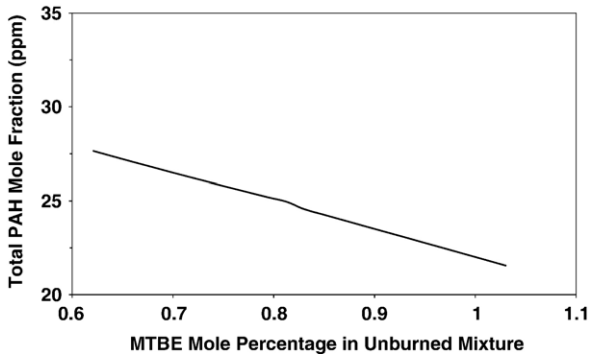

Fig. 6. Effect of MTBE concentration on total PAH amount.

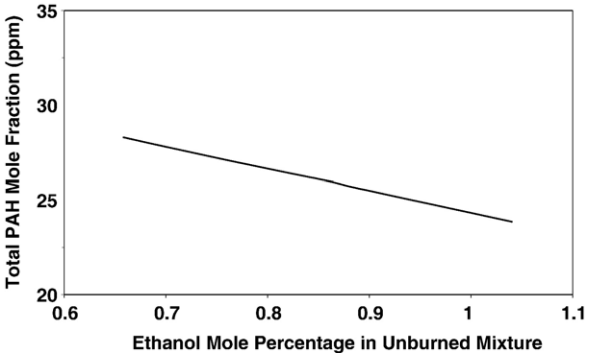

Fig. 7. Effect of ethanol concentration on total PAH amount.

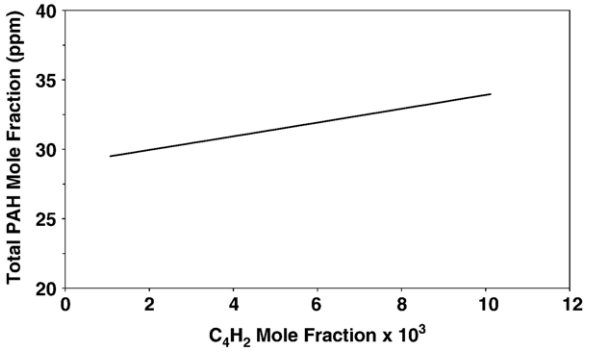

Fig. 9. Effect of C_4H_2 concentration on total PAH amount.

its reverse convert benzene and phenyl to one another. Miller and Melius [37] proposed that the combination of propargyl radicals can also produce benzene or phenyl. In addition to benzene, Marinov et al. [38] suggested that two resonantly stabilized cyclopentadienyl radicals (c-C_5H_5) produced from the unimolecular decomposition of phenoxy radicals combine to form naphthalene. Starting from an initial aromatic structure, the larger PAH can be built by the H-abstraction/C_2H_2-addition mechanism. The addition of aromatic radicals to non-aromatics can also lead to condensed ring compounds [39].

To find the effect of each species concentration on total PAH amount, the sensitivity analysis was carried out. For the *n*-heptane and oxygen amounts equivalence ratio was used as an input parameter. In this analysis, the network was first trained and the connection weights were fixed. After that one by one, each input parameter was varied around its mean value while the other inputs were kept at their mean values. The sensitivity factor for input k is given as

$$S_k = \frac{\sum_{p=1}^{P}\sum_{i=1}^{0}\left(y_{ip}-\overline{y}_{ip}\right)^2}{\sigma_k^2} \quad (2)$$

where $\overline{y}_{ip}$ is the ith output obtained with the fixed weights for the pth pattern, o is the number of network outputs, P is the number of patterns, and σ_k^2 is the variance of the input perturbation [35].

The calculated sensitivity factors are given in Table 3. The effects of some of the important input parameters on predicted total PAH amount are shown in Figs. 5–9. As expected, the equivalence ratio has a strong effect on total PAH amount (Table 3). An increase in equivalence ratio increased the amount of PAH formed (Fig. 5). The addition of fuel oxygenates into a fuel blend affects the flame chemistry by reducing the radical pool and/or producing less reactive reaction intermediates. Although MTBE showed slightly higher influence on total PAH amount, the sensitivity factors for MTBE and ethanol were quite similar under the experimental conditions investigated (Table 3). An increase in oxygenate concentration decreased the PAH amount (Figs. 6 and 7). Among the stable low-molecular-weight aliphatic and single-ring aromatic species, the total PAH amount was significantly more sensitive to changes in vinylacetylene (C_4H_4) and diacetylene (C_4H_2) concentrations (Figs. 8 and 9). Although the dominant reaction pathway is an unresolved issue, C_4 species are known to play an important role in the formation of first aromatic ring and the growth of larger PAH.

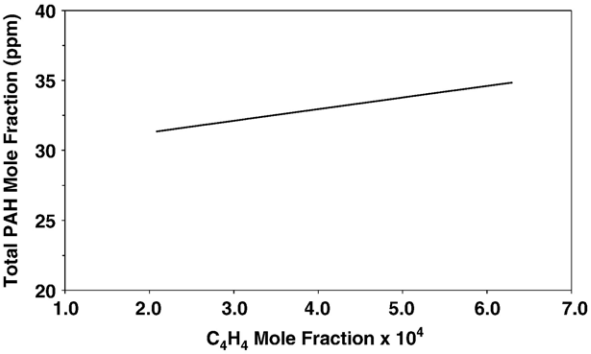

Fig. 8. Effect of C_4H_4 concentration on total PAH amount.

5. Conclusions

In conclusion, the total PAH amount in premixed *n*-heptane and *n*-heptane/oxygenate flames has been predicted using the ANN approach. Although we had limited experimental data the performance of the ANN model developed was satisfactory for both training ($R^2=0.98$) and testing ($R^2=0.98$) sets. The over training or memorization of the network was avoided by the use of a cross-validation set during the training procedure. The results of the sensitivity analysis have shown that the PAH amount is more sensitive to changes in equivalence ratio, and mole fractions of oxygenates and C_4 species. The effects of MTBE and ethanol on PAH amount were comparable. ANN modeling is a useful technique for the prediction of pollutant concentrations. The prediction performance of the network can be further improved by re-training with larger data sets.

Acknowledgment

The support from Izmir Institute of Technology is gratefully acknowledged.

References

[1] P. Boffetta, N. Jourenkova, P. Gustavsson, Cancer risk from occupational and environmental exposure to polycyclic aromatic hydrocarbons, Cancer Causes and Control 8 (1997) 444–472.

[2] A. Bjorseth, T. Ramdahl (Eds.), Handbook of Polycyclic Aromatic Hydrocarbons, Marcel Dekker, New York, 1985.
[3] R. Hagemann, H. Virelizier, D. Gaudin, A. Pesneau, Polycyclic aromatic hydrocarbons in exhaust particles emitted from gasoline and diesel automobile engines, Toxicological and Environmental Chemistry 5 (1982) 227–236.
[4] H.-H. Mi, W.-J. Lee, T.-L. Wu, T.-C. Lin, H.-R. Chao, PAH emission from a gasoline-powered engine, J. Environ. Sci. Health, Part A 31 (1996) 1981–2003.
[5] H.-H. Mi, W.-J. Lee, S.-J. Chen, T.-C. Lin, T.-L. Wu, Effect of gasoline additives on PAH emissions, Chemosphere 36 (1998) 2031–2041.
[6] J.J. Schauer, M.J. Kleeman, G.R. Cass, B.R.T. Simoneit, Measurement of emissions from air pollution sources: 5. C_1–C_{32} organic compounds from gasoline-powered motor vehicles, Environmental Science and Technology 36 (2002) 1169–1180.
[7] B. Zielinska, J. Sagebiel, W.P. Arnott, C.F. Rogers, K.E. Kelly, D.A. Wagner, J.S. Lighty, A.F. Sarofim, G. Palmer, Phase and size distribution of polycyclic aromatic hydrocarbons in diesel and gasoline vehicle emissions, Environmental Science and Technology 38 (2004) 2557–2567.
[8] G.A. Mills, J.S. Howarth, A.G. Howard, The effect of diesel fuel aromaticity on polynuclear aromatic hydrocarbon exhaust emissions, Journal of the Institute of Energy 273 (1984) 273–286.
[9] A.R. Collier, M.M. Rhead, C.J. Trier, M.A. Bell, Polycyclic aromatic compound profiles from a light-duty direct-injection diesel engine, Fuel 74 (1995) 362–367.
[10] H.-H. Mi, W.-J. Lee, C.-B. Chen, H.-H. Yang, S.-J. Wu, Effect of fuel aromatic content on PAH emission from a heavy-duty diesel engine, Chemosphere 41 (2000) 1783–1790.
[11] S.D. Shah, T.A. Ogunyoku, J.W. Miller, D.R. Cocker, On-road emission rates of PAH and *n*-alkane compounds from heavy-duty diesel engines, Environmental Science and Technology 39 (2005) 5276–5284.
[12] P.R. Westmoreland, J.B. Howard, J.P. Longwell, Second Annual Progress Report — Center for Health Effects of Fossil Fuel Utilization, MIT, 1980.
[13] L. Peterca, F. Marconi, Fluorescence spectra and polycyclic aromatic species in a n-heptane diffusion flame, Combustion and Flame 78 (1989) 308–325.
[14] C. Doute, J.L. Delfau, R. Akrich, C. Vovelle, Experimental study of the chemical structure of low-pressure premixed *n*-heptane–O_2–Ar and *iso*-octane–O_2–Ar flames, Combustion Science and Technology 124 (1997) 249–276.
[15] A. El Bakali, J.-L. Delfau, C. Vovelle, Experimental study of 1 atmosphere rich premixed *n*-heptane and *iso*-octane flames, Combustion Science and Technology 140 (1998) 69–91.
[16] A.T. Ingemarsson, J.R. Pedersen, J.O. Olsson, Oxidation of *n*-heptane in a premixed laminar flame, Journal of Physical Chemistry. A 103 (1999) 8222–8230.
[17] F. Inal, S.M. Senkan, Effects of equivalence ratio on species and soot concentrations in premixed *n*-heptane flames, Combustion and Flame 131 (2002) 16–28.
[18] F. Inal, S.M. Senkan, Effects of oxygenate additives on polycyclic aromatic hydrocarbons and soot formation, Combustion Science and Technology 174 (2002) 1–19.
[19] F. Inal, S.M. Senkan, Effects of oxygenate concentration on species mole fractions in premixed *n*-heptane flames, Fuel 84 (2005) 495–503.
[20] C.M. Coats, A. Williams, Investigation of the ignition and combustion of *n*-heptane–oxygen mixtures, Proceedings of the Combustion Institute 17 (1979) 611–621.
[21] C.K. Westbrook, J. Warnatz, W.J. Pitz, A detailed chemical kinetic reaction mechanism for the oxidation of *iso*-octane and *n*-heptane over an extended temperature range and its application to analysis of engine knock, Proc. Combust. Inst. 22 (1988) 893–901.
[22] A. Chakir, M. Bellimam, J.C. Boettner, M. Cathonnet, Kinetic study of *n*-heptane oxidation, International Journal of Chemical Kinetics 24 (1992) 385–410.
[23] E. Ranzi, P. Gaffuri, T. Faravelli, P. Dagaut, A wide-range modeling study of *n*-heptane oxidation, Combustion and Flame 103 (1995) 91–106.
[24] R.P. Lindstedt, L.Q. Maurice, Detailed modeling of *n*-heptane combustion, Combustion Science and Technology 107 (1995) 317–353.
[25] T.J. Held, A.J. Marchese, F.L. Dryer, A semi-empirical reaction mechanism for *n*-heptane oxidation and pyrolysis, Combustion Science and Technology 123 (1997) 107–146.
[26] H.J. Curran, P. Gaffuri, W.J. Pitz, C.K. Westbrook, A comprehensive modeling study of *n*-heptane oxidation, Combustion and Flame 114 (1998) 149–177.
[27] A. El Bakali, J.-L. Delfau, C. Vovelle, Kinetic modeling of a rich, atmospheric pressure, premixed *n*-heptane/O_2/N_2 flame, Combustion and Flame 118 (1999) 381–398.
[28] A. Elkamel, S. Abdul-Wahab, W. Bouhamra, E. Alper, Measurement and prediction of ozone levels around a heavily industrialized area: a neural network approach, Advances in Environmental Research 5 (2001) 47–59.
[29] A. Duran, A. de Lucas, M. Carmona, R. Ballesteros, Simulation of atmospheric PAH missions from diesel engines, Chemosphere 44 (2001) 921–924.
[30] A. de Lucas, A. Duran, M. Carmona, M. Lapuerta, Modeling diesel particulate emissions with neural networks, Fuel 80 (2001) 539–548.
[31] D. Karonis, E. Lois, F. Zannikos, A. Alexandridis, H. Sarimveis, A neural network approach for the correlation of exhaust emissions from a diesel engine with diesel fuel properties, Energy Fuels 17 (2003) 1259–1265.
[32] F. Inal, G. Tayfur, T.R. Melton, S.M. Senkan, Experimental and artificial neural network modeling study on soot formation in premixed hydrocarbon flames, Fuel 82 (2003) 1477–1490.
[33] R.R. Jensen, S. Karki, H. Salehfar, Artificial neural network-based estimation of mercury speciation in combustion flue gases, Fuel Processing Technology 85 (2004) 451–462.
[34] W.L. Fitch, A.D. Sauter, Calculation of relative electron impact total ionization cross sections for organic molecules, Analytical Chemistry 55 (1983) 832–835.
[35] J.C. Principe, N.R. Euliano, W.C. Lefebvre, Neural and Adaptive Systems: Fundamentals Through Simulations, John Wiley & Sons, New York, 1999.
[36] M. Frenklach, H. Wang, Soot Formation in Combustion, in: H. Bockhorn (Ed.), Springer-Verlag, Berlin Heidelberg, Germany, 1994, pp. 165–192.
[37] J.A. Miller, C.F. Melius, Kinetic and thermodynamic issues in the formation of aromatic compounds in flames of aliphatic fuels, Combust. Flame 91 (1992) 21–39.
[38] N.M. Marinov, W.J. Pitz, C.K. Westbrook, A.M. Vincitore, M.J. Castaldi, S.M. Senkan, C.F. Melius, Aromatic and polycyclic aromatic hydrocarbon formation in a laminar premixed *n*-butane flame, Combustion and Flame 114 (1998) 192–213.
[39] J.D. Bittner, J.B. Howard, Composition profiles and reaction mechanisms in a near-sooting premixed benzene/oxygen/argon flame, Proceedings of the Combustion Institute 18 (1981) 1105–1116.